A global lithospheric magnetic field model with reduced noise level in the Polar Regions

Vincent Lesur[1,2] and Stefan Maus[3,4]

Received 18 March 2006; revised 17 May 2006; accepted 23 May 2006; published 4 July 2006.

[1] Due to persistent ionospheric current systems at high latitudes, satellite magnetic measurements have high noise levels in the Polar regions. Consequently, small-scale lithospheric features are much more difficult to resolve there than at lower latitudes. Using linear combinations of spherical harmonics (SH), we define localized functions which are band-limited to a given maximum degree. Thus, a model's SH resolution can be varied over the globe. We produce a lithospheric field model from CHAMP satellite data which resolves features to SH degree 90 at low latitudes, but only to SH degree 60 in the Polar regions. The new model can be downward continued from satellite altitude to the Earth's surface without generating spurious high-latitude anomalies. **Citation:** Lesur, V., and S. Maus (2006), A global lithospheric magnetic field model with reduced noise level in the Polar Regions, *Geophys. Res. Lett.*, *33*, L13304, doi:10.1029/2006GL025826.

1. Introduction

[2] The German CHAMP satellite launched in 2000 has provided more than five years of high-quality scalar and vector magnetic data [*Reigber et al.*, 2002]. The accuracy of the instruments, the low altitude and the long duration of the mission have greatly benefited the mapping of the lithospheric magnetic field (see *Langel and Hinze* [1998] for a review of earlier models). Two distinct approaches have been used for this modelling effort: either the magnetic fields generated by other sources are co-estimated with the lithospheric field, or these fields are filtered out before the modelling by careful selection and processing of the data. The comprehensive model CM4 [*Sabaka et al.*, 2004] is an example of the former approach. Its lithospheric part extends up to spherical harmonic (SH) degree 65. The second approach is focused on the lithosphere alone, with the MF4 model [*Maus et al.*, 2006] as an example. The MF4 model is realistic up to SH degree 80 but includes terms up to maximum SH degree 90. A regularisation has been used during the model estimation, such that the absolute values of the high-degree model coefficients remain reasonably small. Despite this regularization, it is clear when downward continuing MF4 to the Earth's surface, that the model contains unrealistic short wavelength signals in the Polar regions.

[3] In the present work we use the data set processed and selected for building the MF4 model. Contrary to MF4 or CM4, we do not use the usual SH analysis of the magnetic field generated by the lithosphere but use an alternative approach based on localized functions [*Lesur*, 2006] that have similarities with harmonic-splines [*Shure et al.*, 1982] and wavelets [*Freeden et al.*, 1998]. To the authors' knowledge, the only other recent global lithospheric model available that is not based on a SH analysis is that of *Thébault* [2006]; Thébault combines a series of local models built from a Revised Spherical Cap Harmonic Analysis (R-SCHA [*Thébault et al.*, 2006]) to ultimately obtain a global model of the lithospheric magnetic field. The technique we present here is very different. The inversion process based on our localized representation is able to output exactly the model that would be obtained with the usual SH analysis. Indeed, such a model is not robust above SH degree 60 and therefore requires some sort of regularisation. We take advantage of the flexibility of the localized representation to introduce a new kind of regularisation technique to derive a model, very similar to MF4, which has a realistic behaviour even when downward continued to the Earth's surface.

[4] This manuscript is organized as follows: First, in Section 2, a short description of the data selection and processing steps is given, followed in Section 3 by the system of representation and the regularisation techniques. In Section 4, the resulting model is described and compared with MF4.

2. Data Selection

[5] The data set used for this study is identical to the one used for producing the MF4 crustal field model [*Maus et al.*, 2006]. All data are from the polar orbiting CHAMP satellite launched in July 2000 [*Reigber et al.*, 2002]. From an initial altitude of 456 km, CHAMP has descended to 360 km over a period of five years. The magnetic field intensity is measured by an absolute Overhauser Magnetometer while vector measurements are made by a tri-axial Fluxgate Magnetometer. To avoid high-latitude disturbances by field-aligned currents, vector data were not used at magnetic latitudes above 65°.

[6] The satellite measurements were processed as follows:

[7] 1. Subtraction of the field model POMME-2.5 [*Maus et al.*, 2005], which includes the main field to SH degree 15, time averaged degree 2 magnetospheric fields in SM and GSM reference frames, IMF-By correlated fields [*Lesur et al.*, 2005], and magnetospheric ring current fields tracked by the Est/Ist index [*Maus and Weidelt*, 2004].

[1]British Geological Survey (NERC), Edinburgh, UK.
[2]Now at GeoForschungsZentrum Potsdam, Potsdam, Germany.
[3]Cooperative Institute for Research in Environmental Sciences, University of Colorado, Boulder, Colorado, USA.
[4]Also at National Geophysical Data Center, NOAA, Boulder, Colorado, USA.

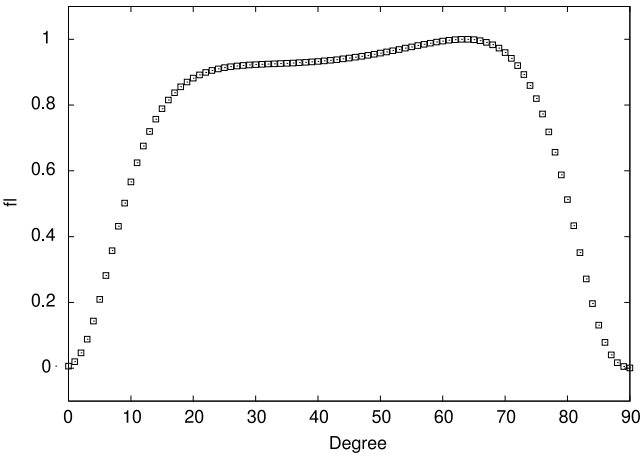

Figure 1. The local functions are defined in equation (2) as weighted sums of products of spherical harmonics. The weights f_l are plotted here against degree for $L = 90$. They are independent of the order.

[8] 2. Subtraction of predictions of the ocean tidal magnetic fields [*Kuvshinov and Olsen*, 2005].

[9] 3. Fitting and subtraction of corrections for degree-1 external and induced fields, including a correction of the low latitude tracks for the far-field effect of the polar electrojets.

[10] 4. Selection of the night time most quiet 70% of the low-latitude data and 5% of the high latitude scalar data.

[11] 5. Application of a line leveling algorithm to reduce offsets between neighboring and overlapping tracks.

[12] This resulted in 3,909,000 scalar and 907,000 vector data. To compute the scalar partial derivatives, which are needed to assemble the normal equations, we use the directions given by the main field model POMME-2.5. Further details of the data selection and processing are given in the MF4 model paper [*Maus et al.*, 2006].

3. Modelling Techniques

[13] We build a magnetic field model of the lithosphere that is not based on the usual SH analysis technique but based on localized functions. However, the system of representation is such that the equivalent Gauss coefficients of the SH representation can be obtained via a direct formula and therefore our final model, just as MF4, is given in terms of Gauss coefficients. Details of the localized functions are given by *Lesur* [2006] and only a short description is given here.

3.1. Model Parameterisation

[14] The magnetic field generated by the lithosphere at satellite altitude, is the gradient of a scalar potential ($\mathbf{B} = -\nabla \mathbf{V}(\theta, \phi, \mathbf{r}, \mathbf{t})$). The potential itself is given in terms of $(L + 1)(2L + 1)$ functions $F_{ij}^L(\theta, \phi, r)$:

$$V(\theta, \phi, r, t) = \sum_{i=1}^{L+1} \sum_{j=1}^{2L+1} \tilde{g}_{ij}(t) F_{ij}^L(\theta, \phi, r) \tag{1}$$

where the functions $F_{ij}^L(\theta, \phi, r)$ are defined by:

$$F_{ij}^L(\theta, \phi, r) = a \sum_{l=1}^{L} \sum_{m=-l}^{l} \left(\frac{a}{r}\right)^{l+1} f_l Y_l^m(\theta_i, \phi_j) Y_l^m(\theta, \phi) \tag{2}$$

where $f_l \neq 0$, $r \geq a$, and $a = 6371.2$ km is the traditional magnetic reference radius. All the functions $F_{ij}^L(\theta, \phi, r)$ have the same basic shape and are symmetric relative to the vector pointing from the coordinate system origin in the direction (θ_i, ϕ_j) of their centre. Their centre positions are given by:

$$\theta_i = \arccos(x_i) \tag{3}$$

$$\phi_j = \frac{2\pi j}{(2L + 1)} \tag{4}$$

where x_i is the ith zero of the Legendre polynomial $P_{L+1}(x)$. The $Y_l^m(\theta, \phi)$ are the usual Schmidt semi-normalized spherical harmonics; Negative orders ($m < 0$) are associated with sin ($m\,\theta$) terms, whereas zero or positive orders ($m \geq 0$) are associated with cos ($m\,\theta$) terms. The f_l in equation (2) are optimised such that the gradient of the functions $F_{ij}^L(\theta, \phi, r)$ decreases as rapidly as possible with the angular distance from their centre. Figure 1 shows the calculated f_l values for a maximum SH degree 90. Also shown, in Figure 2, is the amplitude of the gradient of $F_{ij}^L(\theta, \phi, r)$ as a function of the angular distance from its centre. Any scalar potential given by equation (1) can be modelled in terms of SH with the usual equation

$$V(\theta, \phi, r) = a \sum_{l=1}^{L} \sum_{m=-l}^{l} \tilde{g}_l^m \left(\frac{a}{r}\right)^{l+1} Y_l^m(\theta, \phi) \tag{5}$$

Conversely, because $(2l + 1)(l + 1)$ functions with their centres defined in equations (3) and (4) are used, any scalar potential given by equation (5) can be parameterised as in equation (1). By equating equations (1) and (5), using the

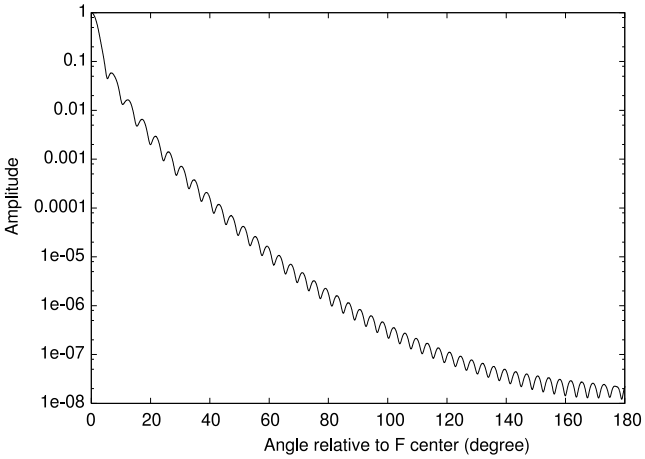

Figure 2. Since the magnetic field vector is the (negative) gradient of the potential, the amplitude of the gradient of $F_{ij}^L(\theta, \phi, a)$ as a function of the angular distance from its centre is presented here.

function definitions in equation (2), multiplying both sides by $Y_{l'}^{m'}(\theta, \phi)$ and integrating over the sphere, it is straightforward to find the relation giving the Gauss coefficients as a function of the $\tilde{g}_{ij}$ at the reference radius:

$$\tilde{g}_{l'}^{m'} = \sum_{i=1}^{L+1} \sum_{j=1}^{2L+1} \tilde{g}_{ij} f_{l'} Y_{l'}^{m'}(\theta_i, \phi_j) \tag{6}$$

The transformation inverse (i.e., a formula giving a possible set of $\tilde{g}_{ij}$ as a function of the Gauss coefficients) is presented by *Lesur* [2006]. For a given potential $V(\theta, \phi, r)$, there is more than one possible set of coefficients $\tilde{g}_{ij}(t)$. This is simply because $(L + 1)(2L + 1)$ functions are needed to parameterise the potential in equation (1) whereas only $L(L + 2)$ spherical harmonics are needed in equation (5). Clearly, some sort of regularisation has to be introduced to find the $\tilde{g}_{ij}$ in equation (1) from a set of magnetic measurements. We usually seek the minimum norm solution by removing zero eigenvalues and the associated eigenvector of the normal equation matrix.

3.2. Regularisation Techniques

[15] We want to produce a model similar to MF4 and use equation (1) to represent the magnetic potential of the lithosphere with localized functions of maximum SH degree 90. There is no advantage in using the localized functions if their flexibility is not used to obtain a solution that differs from the classic SH solution. In this application we use their flexibility in two ways.

[16] First, we introduce over the poles localized functions with a maximum SH degree $L' = 60$ that is smaller than the maximum SH degree $L = 90$ used at mid and low latitudes. It was stated above that the f_l in equation (2) should not be zero. This condition was introduced to ensure that the equivalence between equations (1) and (5) holds. If the functions at high latitude are such that $f_l = 0$ for $l = 61, 62, \cdots, 90$ then it is still possible to represent the obtained scalar potential using SH, as in equation (5), but the converse is no longer true, i.e., there exist potentials defined by equation (5) with SH degree 90 features close to the pole that cannot be represented exactly using equation (1). Since the definition of the functions changes depending on their centre position, we introduce f_l^{ij} values and equation (2) is rewritten as

$$F_{ij}^{L}(\theta, \phi, r) = a \sum_{l=1}^{L} \sum_{m=-l}^{l} \left(\frac{a}{r}\right)^{l+1} f_l^{ij} Y_l^m(\theta_i, \phi_j) Y_l^m(\theta, \phi) \tag{7}$$

For the functions to maximum SH degree 60, the f_l^{ij} have been found by optimization, as before, such that the gradients of the localized functions vanish rapidly away from the function centre. Relation (6), that gives the Gauss coefficients as a function of the $\tilde{g}_{ij}$, is now:

$$\tilde{g}_{l'}^{m'} = \sum_{i=1}^{L+1} \sum_{j=1}^{2L+1} \tilde{g}_{ij} f_{l'}^{ij} Y_{l'}^{m'}(\theta_i, \phi_j) \tag{8}$$

[17] Second, during the inversion process to suppress North/South oriented strips at mid and low latitudes, we smooth the magnetic field model by minimising the integral, given in equation (9), of the second derivative in longitude of its vertical component, squared.

$$I = \int_{\Omega} \left\{ \partial_{\phi}^2 \tilde{B}_z \right\}^2 d\Omega \tag{9}$$

where Ω is the entire spherical surface at reference radius a and $\tilde{B}_z$ is defined as

$$\tilde{B}_z = \sum_{\{i,j\}} \tilde{g}_{ij} \partial_r F_{ij}^{L}(\theta, \phi, r)|_{r=a} \tag{10}$$

In equation (10), the sum is over all the functions that have their centre at mid and low latitudes. Using the function definition in equation (7) and the orthogonality of SH, we obtain

$$I = \sum_{\{i,j\}} \sum_{\{t,s\}} \tilde{g}_{ij} \tilde{g}_{ts} \sum_{l,m} \frac{4\pi a^2}{2l+1} (l+1)^2 f_l^{ij} f_l^{ts} m^4 Y_l^m(\theta_i, \phi_j) Y_l^m(\theta_t, \phi_s) \tag{11}$$

The inner sum gives the element $(\{i, j\}, \{t, s\})$ of the damping matrix. All the other elements of the damping matrix are set to zero. The factor m^4 in the damping matrix elements clearly shows that by minimising the integral (11), are minimised primarily the sectorial terms in the equivalent SH representation of the lithosphere magnetic field model. Since the localized functions are all the same at mid and low latitudes, the f_l^{ij} are equal to the f_l^{ts} in equation (11).

[18] These two regularisation techniques are however not sufficient to ensure that there is a unique solution (i.e., a unique set of $\tilde{g}_{ij}$) to be estimated from the data. The minimum norm solution is therefore chosen, as described above in section 3.1. The inverse problem becomes linear by assuming that the scalar data are the projection of the crustal field vector onto the main field direction. Thus, only one iteration of a damped least square fit is necessary to obtain the solution described in the next section. The value of the damping parameter (i.e., the amount of smoothing applied at mid and low latitudes) is found by trial and error and is set to 1×10^{-12}.

[19] The number of unknown coefficients in this inverse problem is $(L + 1)(2L + 1) = 16471$. However, the problem has necessarily less than $L(L + 2) = 8280$ degrees of freedom, as given by the number of Gauss coefficients of a SH expansion to degree 90. Redundant linear combinations of coefficients can be identified by their zero eigenvalues in the inverse problem. Discarding further small eigenvalues leads to a regularized solution. In the present case, the largest eigenvalue is 1.4×10^{-3} and we accept all eigenvalues larger than 10^{-16}. This results in 7577 eigenvalues, which is, as expected, smaller than the 8280 degrees of freedom of the SH degree 90 inverse problem.

4. Result and Discussion

[20] Using localized functions band limited to SH degree 90 at low latitudes and degree 60 at high latitudes, we have generated a new lithospheric magnetic field model. The vertical component of the new model at the equatorial Earth radius is compared with MF4 for low latitude and polar

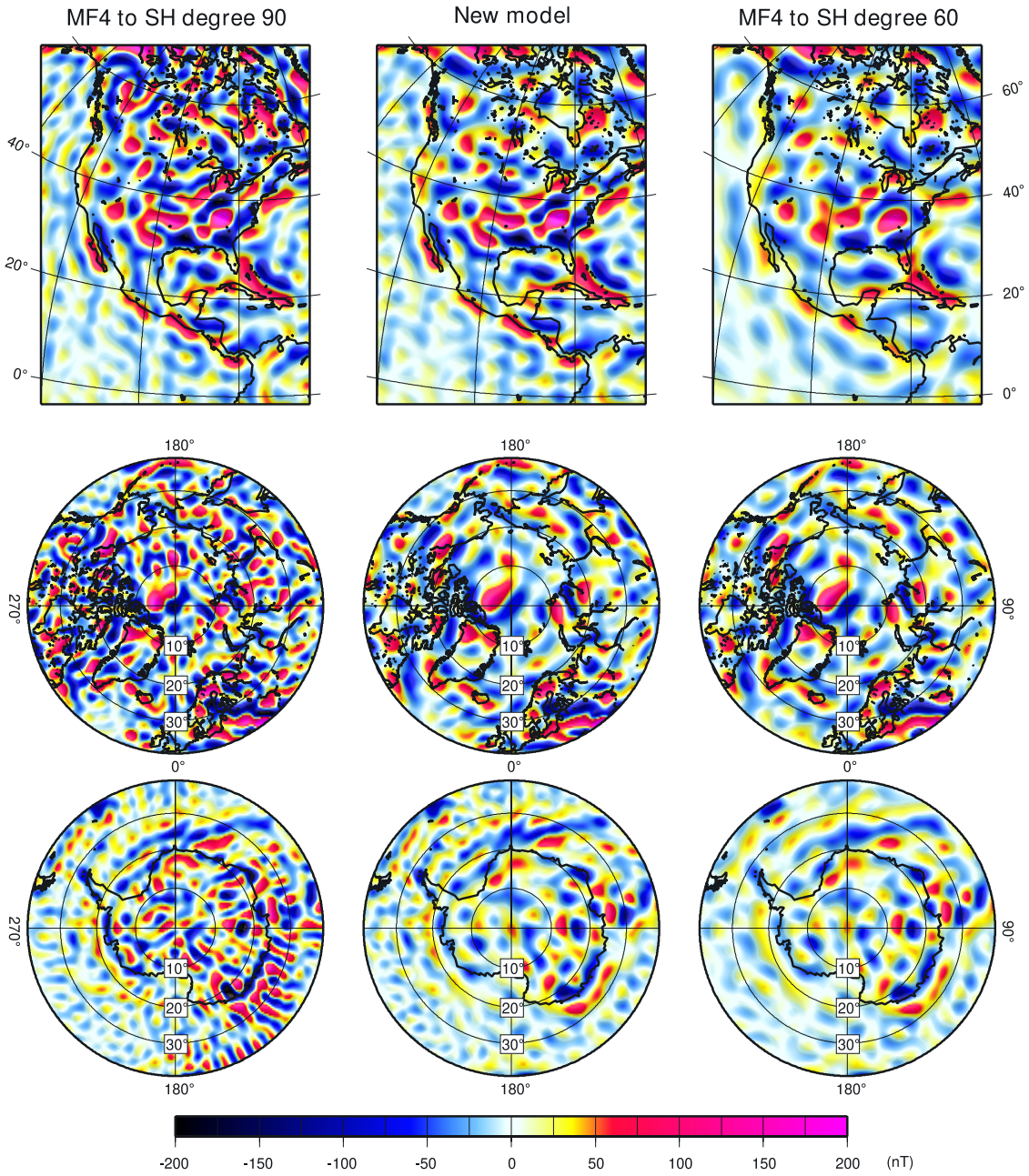

Figure 3. The central column shows the vertical magnetic field component of our new model at the Earth's equatorial radius for a low latitude and the North and South Polar regions. For comparison, the left column shows MF4 in full resolution and the right column shows MF4 limited to SH degree 60. As designed, the new model has the full resolution of MF4 at low latitudes and is band-limited to SH degree 60 in the Polar regions.

regions in Figure 3. At low latitudes, the new model closely resembles the MF4 model to SH degree 90. In the Polar regions, on the other hand, the new model is very similar to MF4 when the latter is displayed only to SH degree 60. Thus, the model avoids the small-scale noise in the Polar regions, while fully resolving the small-scale features at low latitudes. Here, we have defined the Polar regions as above 65° magnetic latitude, where the auroral electrojets have a strong impact on noise levels.

[21] The localized functions used here still have a significant lateral extent. By trial and error we find that to limit the bandwidth to SH degree 60 at magnetic latitudes larger than 65°, the functions to SH degree 90 can be used only for centres located below 40° magnetic latitude. This corresponds to a 25° lateral extent of the function gradients. As seen in Figure 2, the gradients (which are ultimately responsible for the strength of the magnetic field) drop off to 1/1000 over this distance. It is very encouraging to note that there is a smooth transition from higher to lower resolution and no spurious anomalies or oscillations are visible in the mid latitude region.

[22] Figure 4 shows the power spectrum of the new model together with the power spectrum of MF4 and CM4. Up to SH degree 60, the power spectrum of the

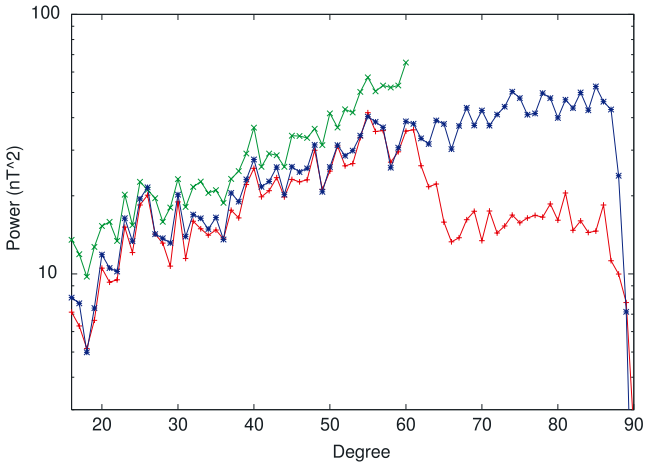

Figure 4. Power spectra from SH degree 16 to 90 of the new model (in red), of CM4 (in green) and MF4 (in blue). The new model is very similar, but not exactly identical, to MF4 at SH degrees smaller than 60. Both models were damped to suppress North/South oriented stripes. For MF4 this regularization was only applied to SH degrees larger than 60. For the new model, on the other hand, such a distinction has not been implemented, resulting in some loss of power in the SH degree 16–60 band.

obtained model is very similar to the MF4 power spectrum but it is significantly reduced from SH degree 60 to 90. The missing power comes mainly from the truncation to degree 60 over the Polar regions but also from the smoothing process at mid and low latitude. This latter regularisation also has an effect at SH degrees smaller than 60. Of course, the power spectrum of the new model does not give a realistic estimate of the lithospheric-field power above SH degree 60. It simply corresponds to a model that does not contain small-scale structure at high latitudes and thus avoids spurious anomalies in the Polar regions. This model is available for download at http://www.gfz-potsdam.de/pb2/pb23/SatMag/litmod4x.html and http://geomag.colorado.edu/MF4x.

[23] **Acknowledgments.** VL thanks NOAA's National Geophysical Data Center for a visiting fellowship, during which this research was carried out. This work was also partly supported by the NERC grant NER/O/S/2003/00677 and is published with the permission of the Executive Director of the British Geological Survey (NERC).

References

Freeden, W., T. Gervens, and M. Schreiner (1998), *Constructive Approximation on the Sphere, With Applications to Geomathematics*, Clarendon, Oxford, U. K.

Kuvshinov, A., and N. Olsen (2005), *3-D Modelling of the Magnetic Field Due to Ocean Tidal Flow*, pp. 359–365, Springer, New York.

Langel, R., and W. Hinze (1998), *The Magnetic Field of the Earth's Lithosphere—The Satellite Perspective*, Cambridge Univ. Press, New York.

Lesur, V., (2006), Introducing localized constraint in global geomagnetic field modelling, *Earth, Planets and Space*, *58*, 477–483.

Lesur, V., S. Macmillan, and A. Thomson, (2005), A magnetic field model with daily variation of the magnetopsheric field and its induced counterpart in 2001, *Geophys. J. Int.*, *160*, 79–88.

Maus, S., and P. Weidelt (2004), Separating the magnetospheric disturbance magnetic field into external and transient internal contributions using a 1D conductivity model of the Earth, *Geophys. Res. Lett.*, *31*, L12614, doi:10.1029/2004GL020232.

Maus, S., S. McLean, D. Dater, H. Luehr, M. Rother, W. Mai, and S. Choi (2005), NGDC/GFZ candidate models for the 10th generation International Geomagnetic Reference Field, *Earth, Planets and Space*, *57*(12), 1151–1156.

Maus, S., M. Rother, K. Hemant, C. Stolle, H. Lühr, A. Kuvshinov, and N. Olsen (2006), Earth's lithospheric magnetic field determined to spherical harmonic degree 90 from CHAMP satellite measurements, *Geophys. J. Int.*, *164*, 319–330, doi:10.111/j.1365-246X.2005.02833.x.

Reigber, C., H. Lühr, and P. Schwintzer (2002), CHAMP mission status, *Adv. Space Res.*, *30*, 129–134.

Sabaka, T., N. Olsen, and M. Purucker (2004), Extending comprehensive models of the Earth's magnetic field with Ørsted and CHAMP data, *Geophys. J. Int.*, *159*, 521–547.

Shure, L., R. Parker, and G. Backus (1982), Harmonic splines for geomagnetic modelling, *Phys. Earth Planet. Inter.*, *28*, 215–229.

Thébault, E. (2006), Global lithospheric magnetic modelling by successive regional analysis, *Earth Planets Space*, *58*, 485–495.

Thébault, E., J. J. Schott, and M. Mandea (2006), Revised spherical cap harmonic analysis (R-SCHA): Validation and properties, *J. Geophys. Res.*, *111*, B01102, doi:10.1029/2005JB003836.

V. Lesur, GeoForschungsZentrum Potsdam, Telegrafenberg, D-14473 Potsdam, Germany. (lesur@gfz-potsdam.de)

S. Maus, Cooperative Institute for Research in Environmental Sciences, University of Colorado, Boulder, CO 80309, USA.